Supporting Information

Nitric Oxide Reversibly Inhibits *Bacillus subtilis* Oxalate Decarboxylase

Mario E. G. Moral, ChingkuangTu, WitchaImaram, Alex Angerhofer, David N. Silverman,

and Nigel G. J. Richards*

Contribution from the Department of Chemistry, University of Florida, Gainesville, FL 32611, the Department of Pharmacology, University of Florida, Gainesville, FL 32610, and the Department of Biochemistry & Molecular Biology, University of Florida, Gainesville, FL 32610.

* Correspondence to Department of Chemistry, Box 117200, University of Florida, Gainesville, Fl 32611-7200, 352-392-3601 (Office); 352-846-2095 (Fax), richards@qtp.ufl.edu.

General Methods

Unless otherwise stated, all chemicals and reagents were purchased from Sigma-Aldrich (St. Louis, MO) or Fisher Scientific (Pittsburgh, PA). (*Z*)-1-(*N*-methyl-*N*-[6-(*N*-methylammoniohexyl)amino]di-azen-1-ium-1,2-diolate (MAHMA NONOate) and diethylammonium (*Z*)-1-(N,N-diethylamino)diazen-1-ium-1,2-diolate were obtained from Cayman Chemical (Ann Arbor, MI). and $^{13}C_2$-oxalic acid (99%) was provided by Cambridge Isotope Laboratories (Andover, MA). DNA primers bearing the C383S point mutation, NdE, and BamHI restriction sites were designed and purchased from Integrated DNA Technologies, Inc. (Coraville, IA). Protein concentrations were determined using a modified Bradford assay kit from Pierce (Rockford, IL), for which standard curves were constructed with bovine serum albumin. The metal content of each purified enzymewas determined by ICP-MS measurements at the University of Wisconsin Soil and Plant Analysis Laboratory, using samples prepared by published procedures (*1*). An OxDC:pET32a plasmid encoding C-terminally, His_6-tagged, WT *Bacillus subtilis*OxDC was generously provided by Dr. Stephen Bornemann (John Innes Centre, Norwich, UK).

Membrane Inlet Mass Spectrometry (MIMS) Measurements

A general description of the mass spectrometer used in the MIMS experiments has been provided elsewhere (*2-4*). Briefly, a Silastic inlet probe from Dow Corning (Midland, MI) (1.5 mm internal diameter and 2.0 mm external diameter) sealed with a glass bead at one end and containing a gas-permeable membrane was interfaced to an Extrel EXM-200 quadrupole mass spectrometer. The probe was immersed in solutions contained in a gas-tight reaction vessel that was maintained at a temperature of 25 ^{o}C as detailed previously (*3*). Mass spectra were obtained using 70 eV electron impact ionization with an emission current close to 1 mA and source pressures were approximately 1 x 10^{-6}torr.Reaction solutions used in the MIMS studies initially contained either unlabeled 50 mMpotassium oxalate or 50mM $^{13}C_2$-labeled oxalate (99%) dissolved in in 50 mM acetate buffer, pH 4.2, containing 0.2% Triton X-100and a trace amount of Antifoam A(final volume 2 mL). Dioxygen was then depleted in these

solutions by purging with He until MIMS analysis showed baseline levels. In the absence of NO, reactions were initiated by the addition of wild type, His_6-tagged OxDC or the C383S OxDC mutant (prepared as described below) so that the final enzyme concentrationswere 1.4 μMand 0.43 μM, respectively. In experiments examining the ability of NO to inhibit OxDC activity, a solution of either 5 mM MAHMA NONOate(final concentration 50 μM NO) (*5*), or 10 mMdiethylammonium (*Z*)-1-(N,N-diethylamino)diazen-1-ium-1,2-diolate(final concentration 75 μM NO) (*6*, *7*), dissolved in 0.01 M aq. NaOH was injected into the reaction vessel 2 min prior to initiation of the reaction by the addition of enzyme. When the reversibility of NO-dependent OxDC inhibition was investigated, either air (15 sec)or pure O_2 (30 sec) was bubbled into the reaction solution.

Expression and Purification of Untagged Recombinant WTOxDC and the C383S OxDC Mutant

The gene encoding the C383S OxDC mutant was obtained from the *Bacillus subtilisYvrk* gene as template by PCR using the appropriate primers, and the resulting amplicon was digested with the NdeIand BamHI restriction enzymes. This gave an DNA fragment that was ligated into the kanamycin-resistant pET9a vector. The resulting C383S plasmid construct was cloned and purified from JM109 *Escherichia coli*by standard methods. After sequencing, the C383S OxDC construct was used to transform BL21/DE3*Escherichiacoli*for protein expression. Both of the untagged enzymes were then expressed and purified using a slight modification of published procedures (*1*) in which fractions from hydrophobic interaction chromatography on phenylsepharose were exhaustively dialyzed against 50 mMTris buffer, pH 8.5, containing 500 mMNaCl.

Expression and Purification of C-terminally His_6-tagged Recombinant WT OxDC

The OxDC:pET-32a plasmid construct for His_6-tagged WT *Bacillussubtilis*OxDC was cloned into BL21/DE3*Escherichiacoli*, and the enzyme was expressed and purified using literature procedures (*8*, *9*) except that cells were lysed using sonication. Pooled OxDC fractions obtained by elution from a Ni-

NTA column (Qiagen, Valencia, CA) were desalted using a Sephadex column equilibrated with 50 mMTris buffer, pH 8.5, containing 500 mMNaCl.

Figure S1MIMS experiment showing the effect of adding MAHMA NONOate to OxDC during catalytic turnover. Helium gas was bubbled into a solution of 50 mM potassium oxalate dissolved in 50 mM sodium acetate buffer, pH 4.2, containing 0.2% Triton X-100 at 25 ^{o}Cto remove other gases prior to the MIMS measurements. After 2 min (during which time He was used to remove gases from the "headspace" above the reaction solution), His_6-tagged, wild type OxDC (final concentration 1.4 μM) was added to initiate reaction. CO_2 generation took place immediately (**red**). After an additional 20 sec, a solution of MAHMA NONOate was injected into the reaction mixture (final NO concentration 50 μM) and NO formation was observed (**blue**). The dioxygen concentration under these conditions was also monitored (**green**). OxDC activity under identical conditions in the absence of NO is also indicated on the MIMS plot (**thin black line**), showing that NO inhibition does not result merely from dioxygen depletion due to chemical reaction and NO_2 formation.

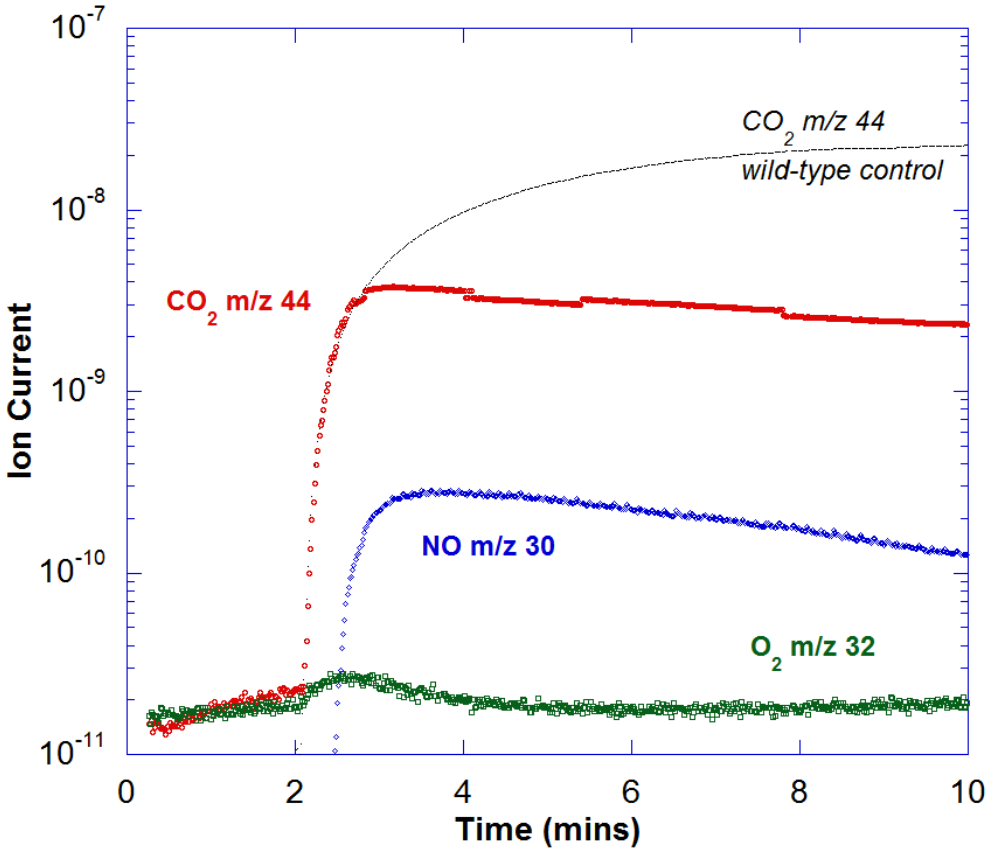

Figure S2: MIMS experiments showing that OxDC inhibition is not dependent on the source of NO. (A) Helium gas was bubbled into a solution of 50 mM potassium oxalate dissolved in 50 mM sodium acetate buffer, pH 4.2, containing 0.2% Triton X-100 at 25 ^{o}Cto remove other gases prior to the MIMS measurements. After 2 min (during which time He was used to remove gases from the "headspace" above the reaction solution), MAHMA NONOate was added to the solution mixture (final concentration 37.5µM) and NO formation was observed (**blue**). After an additional 2 min, catalysis was initiated by the addition of His_6-tagged OxDC (final concentration 1.4µM) and CO_2 production was monitored (**red**). After a further 8 min, pure O_2 (**green**) was bubbled into solution for 30 sec reversing inhibition. (B) Identical experimental conditions except that NO was generatedfrom diethyl-ammonium (Z)-1-(N,N-diethylamino)diazen-1-ium-1,2-diolate(final concentration 50µM).

(A) (B)

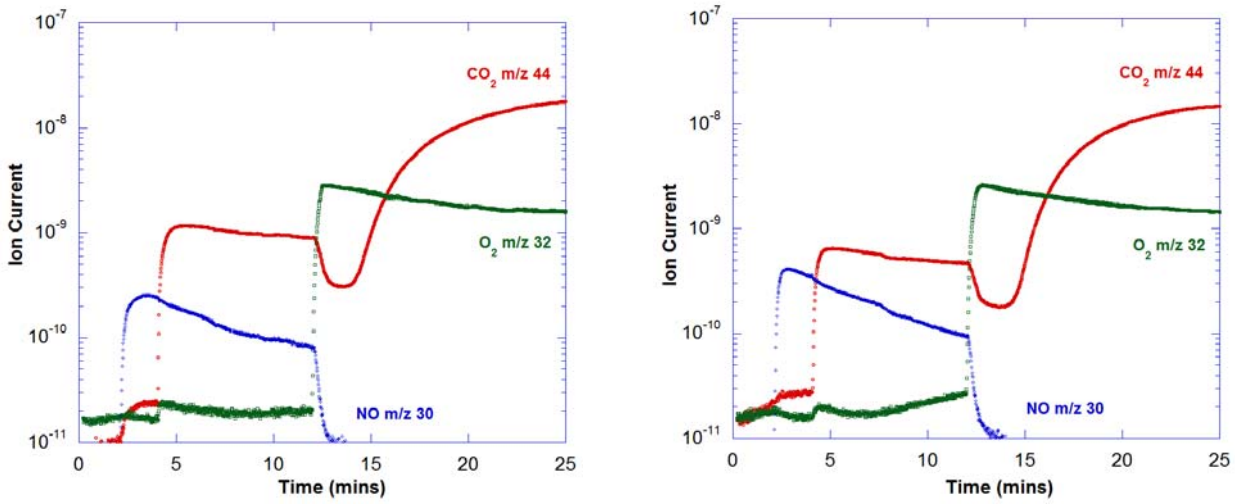

Figure S3MIMS experiment showing reversible inhibition of the C383S OxDC mutant by NO. Helium gas was bubbled into a solution of 50 mM potassium oxalate dissolved in 50 mM sodium acetate buffer, pH 4.2, containing 0.2% Triton X-100 at 25 ^{o}Cto remove other gases prior to the MIMS measurements. After 2 min (during which time He was used to remove gases from the "headspace" above the reaction solution), MAHMA NONOate was added to the solution mixture (final concentration 25 μM) and NO formation was observed (**blue**). After an additional 2 min, catalysis was initiated by the addition of the untagged C383S OxDC mutant (final concentration 0.43 μM) and CO_2 production was monitored (**red**). After a further 8 min, pure O_2 (**green**) was bubbled into solution for 30 sec reversing inhibition. Note the longer lag time observed for the C383S OxDC mutant relative to that seen for the wild type enzyme (Figure S2), which might be due to several factors, including the lower specific activity of this mutant, weaker dioxygen binding and/or reactivity for the C383S OxDC mutant, and tighter NO binding to the mutant enzyme. Work is in progress to elucidate the molecular basis for this intriguing observation.

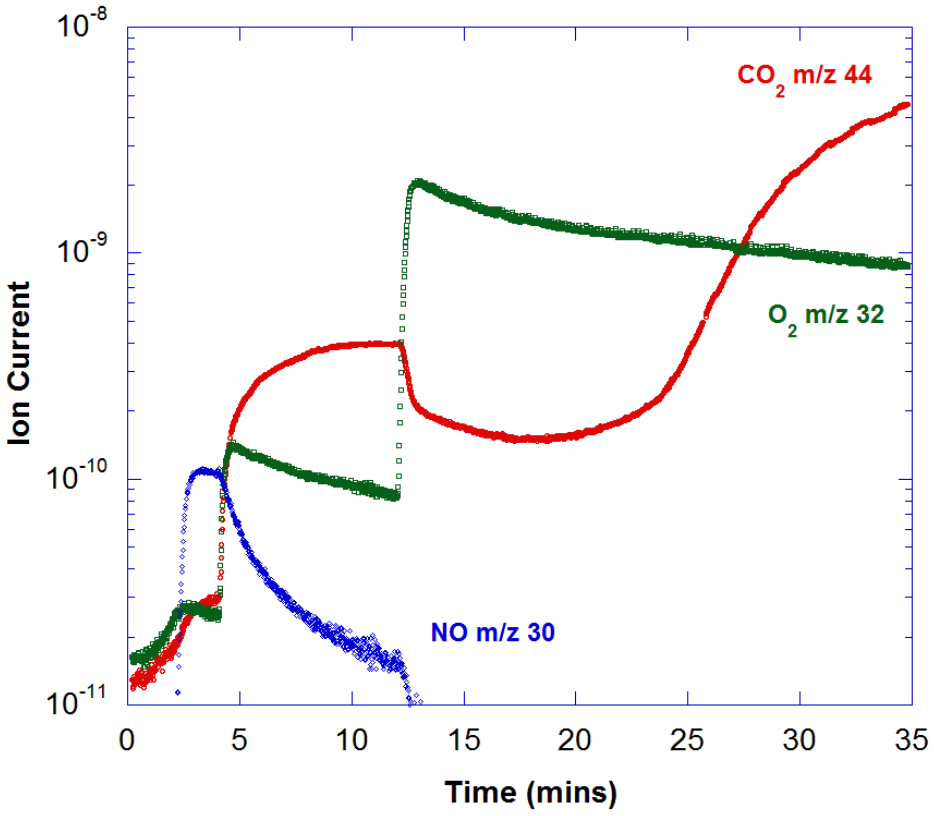

General Procedure for Continuous Wave EPR Measurements

An aliquot of enzyme stock solution (300 μL of approx. 0.14 mM enzyme in 50 mMTris buffer, pH 8.5, containing 500 mMNaCl) was mixed with 2 M potassium acetate buffer, pH 4.1, (18 μL) to give a final buffer concentration of approx. 110 mM. The small amount of enzyme that precipitated on lowering the solution pH was then removed by centrifugation (14,850 rpm, 5 min) and the resulting clear supernatant was collected (pH 4.5) and employed in subsequent EPR experiments after degassing with argon (care was taken to prevent excessive foaming) for 1 min in an anaerobic chamber (dry box flooded with N_2(g)) under a nitrogen atmosphere. This procedure reduced the solution volume to 240 μL. An aliquot (120 μL) of this "stock" enzyme solution was then transferred to a quartz tube (3 mm internal diameter and 4 mm external diameter), which was capped and rapidly frozen in cold isopentane (pre-cooled to near its freezing point in liquid N_2). The cold sample tube was placed in a pre-cooled cryostat (Oxford ESR900) for CW EPR measurements (Figure 3, spectrum (A)). After subsequent thawing of the degassed sample (in the anaerobic chamber), the tube was opened under N_2(g) atmosphere prior to addition of the NO donor. 13 μL of 10 mM degassed MAHMA NONOate in 10 mM aq. NaOH was then added to the enzyme-containing solution in the EPR tube and allowed to react for 5 min before the sample tube was re-capped and rapidly frozen using pre-cooled isopentane. CW EPR measurements were then performed as before (Figure 3, spectrum (B)). After thawing, the solution pH of the sample was determined to be 4.6.The remaining degassed "stock" OxDC solution (approximately 120 μL) in 110 mM acetate buffer was then subject to a similar set of procedures as outlined above except that potassium oxalate (14 μL of a 100 mM oxalate solution in acetate buffer, pH 4.1) was added as well as 1 mM MAHMA NONOate prior to cooling and CW EPR measurements (Figure 3, spectrum (C)). A "blank" sample was also prepared using 20 mM metal-free Tris buffer, pH 8.5, which was subjected to identical treatment as the NO-exposed solution of OxDC (Figure 3, spectrum (D)). Additional control CW EPR spectra were obtained for the 20 mM metal-free Tris buffer, pH 4.1, and a solution of

MAHMA NONOate in 10 mM aq. NaOH. These experiments were designed to reveal the potential binding of dissolved NO to those Mn sites which were accessible to X-band EPR analysis through changes in their fine structure values.

All EPR spectra were recorded at liquid helium temperature, using a commercial BrukerElexsys E580 spectrometer with the standard rectangular TE_{102} resonator. Instrumental parameters were: 90 kHz modulation frequency, 15 G modulation amplitude, 0.6 mW microwave power, 9.4347 GHz microwave frequency, 330 ms time constant, and 330 ms conversion time/point. Each spectrum consisted of a single scan of 5001 data points over a scan range of 50 to 7050 G.

Simulations of the X-band EPR Spectra for the Mn(II) Sites in OxDC

In an effort to ascertain the extent to which the X-band EPR spectrum of wild type OxDC is sensitive to contributions from the Mn(II) site exhibiting the smaller fine structure constant *D*, we performed simulations with the "easyspin" toolbox for MatLab (*10*) using published parameter values (Figures S4 and S5) (*11*, *12*). These simulations showed that the relative intensities of the lines associated with the Mn(II) center exhibiting the smaller fine structure parameter $|D|$ are much larger than those for the other. Consequently, NO binding to the Mn(II) site with the larger $|D|$ value would lead only to minimal changes in the observed X-band EPR powder spectrum ofOxDC.

Figure S4Simulations of the two Mn(II) sites in OxDC using fine structure values determined by high-field EPR, as reported by Angerhofer et al (*11*). EPR spectra were simulated using the **fieldmod** routine of the "easyspin" toolbox for MatLab (10) witha modulation amplitude of 1.0 mT. The black trace shows the sum of both Mn(II) sites before applying the field modulation, and therefore it does not represent the sum of the individual demodulated EPR spectra for the N- and C-terminal sites. Magnetic Parameters used for both sites: g_{iso} = 2.00088, A_{iso} = 253 MHz. Fine structure parameters used for the N-terminal site: D = 2150 MHz, E = 110 MHz, with D- and E-strain values being set to 0.6 of D and E, respectively. Fine structure parameters used for the C-terminal site: D = -1200 MHz, E = 250 MHz, with D- and E-strain values being set to 0.4 of D and E, respectively.

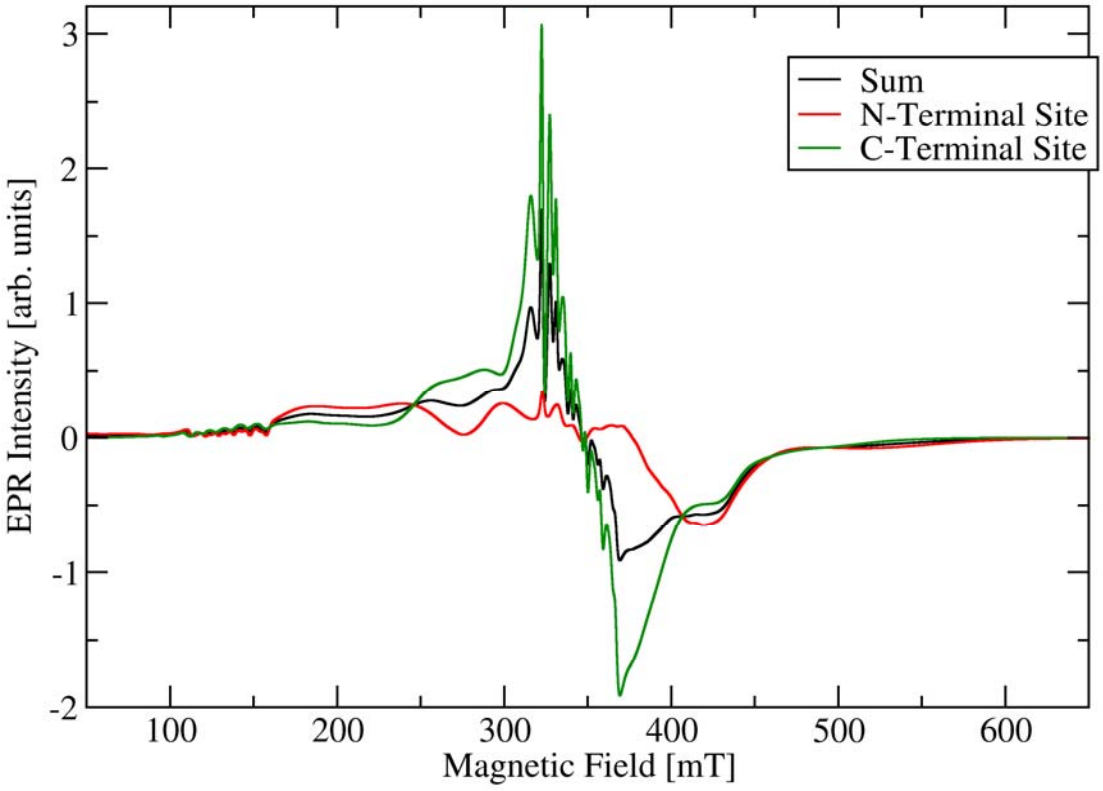

Figure S5Simulations of the two Mn(II) sites in OxDC using fine structure values determined by high-field EPR, as reported by Tabares et al (*12*). EPR spectra were simulated using the **fieldmod** routine of the "easyspin" toolbox for MatLab (10) witha modulation amplitude of 1.0 mT. The black trace shows the sum of both Mn(II) sites before applying the field modulation, and therefore it does not represent the sum of the individual demodulated EPR spectra for the N- and C-terminal sites. Magnetic Parameters used for both sites: g_{iso} = 2.00088, A_{iso} = 253 MHz. Fine structure parameters used for the N-terminal site: D = -1350 MHz, E = 230 MHz, with D- and E-strain values being set to 0.4 of D and E, respectively. Fine structure parameters used for the C-terminal site: D = 4170 MHz, E = 720 MHz, with D- and E-strain values being set to 0.4 of D and E, respectively.

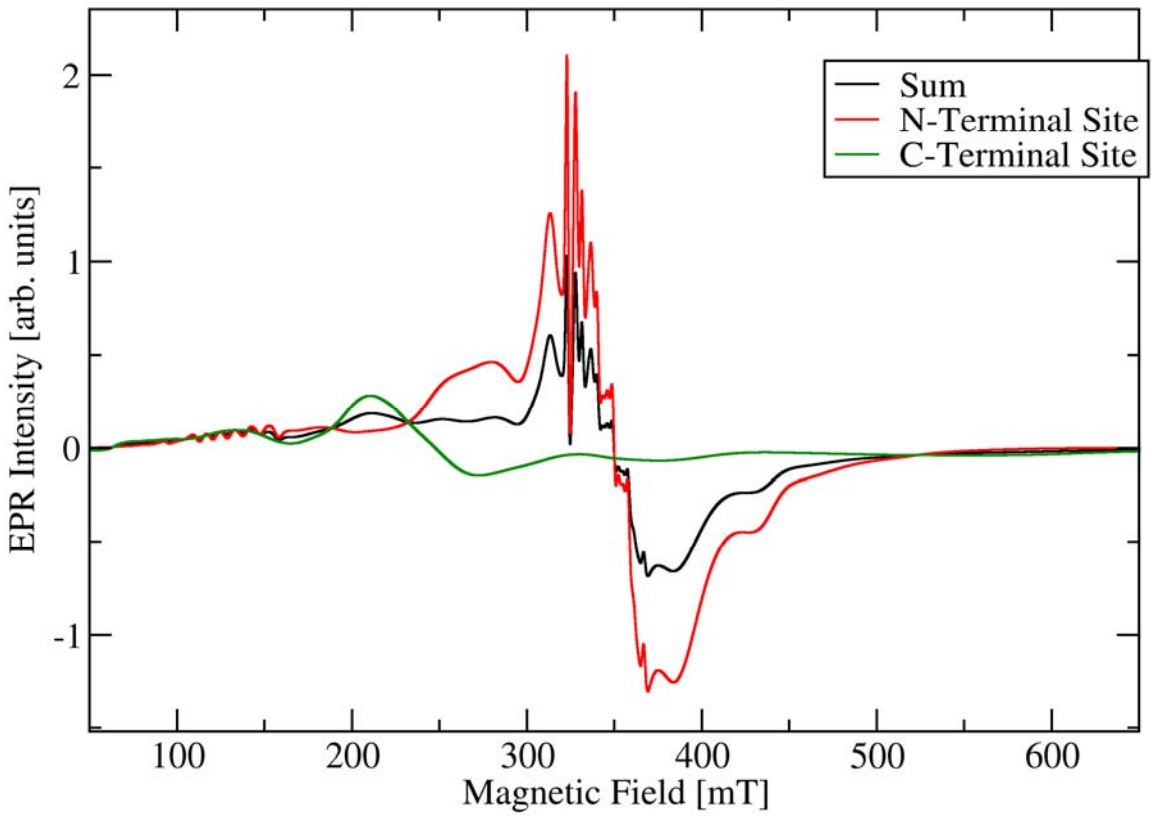

Literature Cited

1. E. W. Moomaw, A. Angerhofer, P. Moussatche, A. Ozarowski, I. Garcia-Rubio and N. G. J. Richards, *Biochemistry*, 2009, **48**, 6116.

2. R. Mikulski, C. K. Tu, E. R. Swensen and D. N. Silverman, *Free Rad. Biol. Med.*, 2010, **48**, 325.

3. C. K. Tu, E. R. Swensen and D. N. Silverman, *Free Rad. Biol. Med.*, 2007, **43**, 1453.

4. D. N. Silverman, *Methods Enzymol.*, 1982, **87**, 732.

5. J. A. Hrabie, J. R. Klose, D. A. Wink and L. K. Keefer, *J. Org. Chem.*, 1993, **58**, 1472.

6. C. M. Maragos, D. Morley, D. A. Wink, T. M. Dunams, J. E. Saavedra, A. Hoffman, A. A. Bove, L. Isaac, J. A. Hrabie and L. K. Keefer, *J. Med. Chem.*, 1991, **34**, 3242.

7. L. K. Keefer, R. W. Nims, K. M. Davies and D. A. Wink, *Methods Enzymol.*, 1996, **268**, 281.

8. M. R. Burrell, V. J. Just, L. Bowater, S. A. Fairhurst, L. Requena, D. M. Lawson and S. Bornemann, *Biochemistry*, 2007, **46**, 12327.

9. V. J. Just, M. R. Burrell, L. Bowater, I. McRobbie, C. E. Stevenson, D. M. Lawson and S. Bornemann, *Biochem. J.* 2007, **407**, 397.

10. S. Stoll and A. Schweiger, *J. Magn. Reson.* 2006, **178**, 42.

11. A. Angerhofer, E. W. Moomaw, I. Garcia-Rubio, A. Ozarowski, J. Krzystek, R. T. Weber and N. G. J. Richards, *J. Phys. Chem. B*, 2007, **111**, 5043.

12. L. C. Tabares, J. Gätjens, C. Hureau, M. R. Burrell, L. Bowater, V. L. Pecoraro, S. Bornemann and S. Un, *J. Phys. Chem. B*, 2009, **113**, 9016.